Cancer Cell
Article

The *p53* mRNA-Mdm2 Interaction Controls Mdm2 Nuclear Trafficking and Is Required for p53 Activation following DNA Damage

Madhavsai Gajjar,[1,4] Marco M. Candeias,[1,4] Laurence Malbert-Colas,[1] Anne Mazars,[1] Jun Fujita,[2] Vanesa Olivares-Illana,[1,3,*] and Robin Fåhraeus[1,*]
[1]Cibles Therapeutiques, INSERM Unité 940, Institut de Génétique Moléculaire, Université Paris 7, IUH Hôpital St. Louis, 75010 Paris, France
[2]Department of Clinical Molecular Biology, Graduate School of Medicine, Kyoto University, Kyoto 606-8507, Japan
[3]Present address: Instituto de Fisica, Universidad Autonoma de San Luis Potosi, 78290 SLP, Mexico
[4]These authors contributed equally to this work
*Correspondence: vanesa.olivares-illana@inserm.fr (V.O.-I.), robin.fahraeus@inserm.fr (R.F.)
DOI 10.1016/j.ccr.2011.11.016

SUMMARY

The ATM kinase and p53 are key tumor suppressor factors that control the genotoxic stress response pathway. The ATM substrate Mdm2 controls p53 activity by either targeting p53 for degradation or promoting its synthesis by binding the *p53* mRNA. The physiological role and regulation of Mdm2's dual function toward p53 is not known. Here we show that ATM-dependent phosphorylation of Mdm2 at Ser395 is required for the *p53* mRNA-Mdm2 interaction. This event also promotes SUMO-conjugation of Mdm2 and its nucleoli accumulation. Interfering with the *p53* mRNA-Mdm2 interaction prevents p53 stabilization and activation following DNA damage. These results demonstrate how ATM activity switches Mdm2 from a negative to a positive regulator of p53 via the *p53* mRNA.

INTRODUCTION

ATM is a key regulator of genome stability and initiator of cellular signaling pathways required for the DNA damage response. Mutations in ATM cause ataxia telangiectasia and result in the development of cancers. Activation of ATM following double-stranded DNA break involves its autophosphorylation and monomerization and leads to phosphorylation of DNA damage checkpoint proteins, such as p53, Chk2, c-Abl, BRCA-1, and Mdm2 (Bartek et al., 2007; Kitagawa and Kastan, 2005; Shiloh, 2003). Different studies on ATM and the Wip1 phosphatase have shown that phosphorylation and dephosphorylation of p53 on Ser15 and Mdm2 on Ser395 are important for regulating p53 activity (Banin et al., 1998; Canman et al., 1998; Khanna et al., 1998; Lu et al., 2007; Maya et al., 2001).

Activation of p53 in response to stress leads to an early induction of Mdm2. Binding of Mdm2 to the N terminus of p53 promotes either p53 monoubiquitination and nuclear export or p53 polyubiquitination and degradation by the 26S proteasomal pathway (Honda et al., 1997; Li et al., 2003). Mdm2 also has the capacity to regulate *p53* mRNA translation indirectly via its interaction with L26 or directly by binding to the *p53* mRNA (Candeias et al., 2008; Naski et al., 2009; Ofir-Rosenfeld et al., 2008). Direct interaction with the mRNA also accounts for Mdm2's induction of XIAP synthesis (Gu et al., 2009). The *p53* mRNA-Mdm2 interaction is mediated by the C-terminal RING domain of Mdm2 and the *p53* mRNA sequence that encodes the Mdm2 binding site in the N terminus of p53. This interaction also controls Mdm2's E3 ligase activity (Candeias et al., 2008).

Mdm2-dependent regulation of p53 expression and activity is controlled via interactions with a number of different proteins that are linked to the nucleolus. Several ribosomal factors, such as L5, L11, and L23, have been shown to interact with the central region of Mdm2 that contains its acid and zinc domains (Deisenroth and Zhang, 2010). The central region of Mdm2 also binds $p14^{Arf}$, which can retain Mdm2 in the nucleolus

Significance

The presented results show the importance of the *p53* mRNA-Mdm2 interaction in activating p53 following DNA damage and describe an additional function for an mRNA. The *p53* mRNA binding changes Mdm2 activity and prevents Mdm2-mediated ubiquitination of p53 while it stimulates p53 synthesis and promotes Mdm2 nucleolar localization. These results help to explain the previous paradox of why Mdm2 is upregulated by p53 in response to genotoxic stress. As long as the ATM pathway is active, Mdm2 serves as a positive regulator of p53 while it rapidly degrades p53 when the DNA damage response is turned off. These results implicate a route for therapeutic intervention aimed at controlling Mdm2 activity toward p53.

and prevent its export to the cytoplasm (Tao and Levine, 1999; Weber et al., 1999). The localization of Mdm2 to nucleoli plays a key role in p53 activation and involves the interaction of Mdm2 with the PML (promyelocytic leukemia) tumor suppressor protein (Bernardi et al., 2004; Boulon et al., 2010; Lohrum et al., 2000; Weber et al., 1999). SUMOylation of PML, or of its interacting partners, helps to target a number of different proteins to PML nuclear bodies that are linked to a variety of different stress and damage pathways that control transcription and translation regulation, tumor suppression, DNA repair, and apoptosis (Bernardi and Pandolfi, 2007; Heun, 2007; Lallemand-Breitenbach and de Thé, 2010).

Here we investigated the physiological role of the *p53* mRNA-Mdm2 interaction in the well-described p53 tumor suppressor pathway triggered by genotoxic stress.

RESULTS

Mdm2 Is Required to Promote p53 Activity following DNA Damage in an ATM-Dependent Manner

Introduction of siRNA against Mdm2 in the human sarcoma cells MLS1765 that express endogenous wild-type p53 (p53wt) resulted in an increase in the number of cells undergoing apoptosis, in line with the notion that Mdm2 is a negative regulator of p53 activity under normal conditions. When MLS1765 cells were exposed to the DNA-damaging agent doxorubicin, the siRNA treatment against Mdm2 instead lead to a decrease in the apoptotic numbers, indicating that Mdm2 helps to activate apoptosis under conditions of genotoxic stress. siRNA against ATM also reduced the amount of cells undergoing apoptosis after doxorubicin treatment, and the strongest inhibition of apoptosis was observed when siRNA for both Mdm2 and ATM was introduced (Figure 1A; Figures S1A–S1C available online). Introduction of exogenous Mdm2 and p53 in the $p53^{-/-}$; $Mdm2^{-/-}$ double-KO (DKO) MEFs resulted in a four times higher rate of p53-dependent apoptosis following induction of DNA double-strand breaks by treating cells with etoposide (Figure 1B).

To further investigate the role of Mdm2 as an activator of the DNA damage-response pathway, we used the p53 null H1299 cell line, in which we introduced p53wt. Altering the levels of Mdm2 by either knocking down endogenous Mdm2 using siRNA or by overexpressing Mdm2 revealed an Mdm2-dependent inhibition of p53-induced apoptosis under normal conditions and an Mdm2-dependent augmented p53-dependent apoptosis in response to genotoxic stress. This proapoptotic effect of Mdm2 was significantly suppressed when the activity of endogenous ATM was diminished by siRNA or by overexpressing the Wip1 phosphatase (Figure 1C). The latter reverses ATM-mediated autophosphorylation and phosphorylation of p53 and Mdm2 (Lu et al., 2007, 2005; Shreeram et al., 2006; Yoda et al., 2008). Treatment of cells with an ATM kinase inhibitor (ATMi) prevented Mdm2 from inducing apoptosis upon doxorubicin treatment (Figure 1D; Figure S1D). Furthermore, we observed that ectopically expressed Mdm2 acted as a negative regulator of apoptosis in doxorubicin-treated cells expressing endogenous p53 and Mdm2 but deficient for ATM (AT5-BIVA cells) but acted as a positive regulator of apoptosis when exogenous ATM was introduced (Figure 1E). Taken together, these results indicate that Mdm2 acts as a positive regulator of p53 activity following genotoxic stress in an ATM-dependent fashion.

Phosphorylation of Mdm2 at Ser395 Induces p53 Activity Independently of the p53-Mdm2 Protein-Protein Interaction

ATM mediates phosphorylation, directly or indirectly, through Chk2 on several residues in the p53 N terminus (Shiloh, 2003), which harbors the *trans*-activating domains and the Mdm2-binding site (Oliner et al., 1993; Zhu et al., 1998). The current model on how phosphorylation at these sites suppresses Mdm2-dependent inhibition of p53 activity suggest that these events prevent the p53-Mdm2 protein-protein interaction (Cheng et al., 2009; Jimenez et al., 1999; Lu et al., 2007; Shieh et al., 1997). This cannot, however, explain our observations that Mdm2 not only stops being an inhibitor of p53 but in fact enhances its activity following genotoxic stress. Hence, other molecular mechanisms must be in place to explain Mdm2's switch from a negative to a positive regulator of p53. To test this hypothesis, we first used the p76 Mdm2 isoform (Mdm2p76), which lacks the N terminus and the capacity to bind the p53 protein (Perry, 2004). Expression of Mdm2p76 stimulated p53-dependent apoptosis following DNA damage in a similar way as the Mdm2wt, demonstrating that inhibition of the p53-Mdm2 protein-protein interaction is not required in order for Mdm2 to enhance p53 activity in response to DNA lesions (Figure 2A; Figure S2A).

Mdm2 is phosphorylated at Ser395 by ATM (Maya et al., 2001) and has been implicated in ATM-dependent activation of p53, so we tested whether the proapoptotic disposition of Mdm2 is dependent on the phosphorylation of Mdm2 at this residue. The introduction of the S395A mutation in Mdm2 caused a significant reduction in apoptosis in AT5-BIVA, H1299, and DKO cells expressing ATM and p53 in the presence of doxorubicin, confirming the importance of this site for p53 activation in response to DNA damage (Figure 2B). In each cell line, we observed a decrease in p53 expression in cells exposed to doxorubicin in the presence of Mdm2Ser395A, as compared to Mdm2wt (Figure S2B). As can be expected, the relative levels of apoptosis and p53 expression varies between cell lines depending on sensitivity to the drug and the levels of p53 expression. The binding of the *p53* mRNA to Mdm2 can stimulate p53 synthesis, and, because Ser395 is situated close to the RING domain, where the ability to bind *p53* mRNA lies, we next assessed whether the *p53* mRNA-Mdm2 interaction plays a role in Mdm2-mediated activation of p53 following DNA damage. We expressed p53wt protein from an mRNA that carries a single silent point mutation (*p53L22L*) and has a low affinity for Mdm2 (Candeias et al., 2008), or we expressed an Mdm2 protein that carries a point mutation that reduces its affinity to RNA (Mdm2G446S) (Elenbaas et al., 1996). Both mutants failed to induce p53-dependent apoptosis in H1299 cells treated with doxorubicin and, in fact, p53wt protein expressed from the *p53L22L* mRNA was unable to induce a significant amount of apoptosis in the presence of Mdm2wt (Figure 2C). On the contrary, introduction of the phospho-mimetic Mdm2S395D mutant caused an increase in apoptosis as compared to Mdm2wt. In addition, similar to what was observed in AT5-BIVA and DKO cells, the level of p53 was low in H1299 cells in which the *p53*

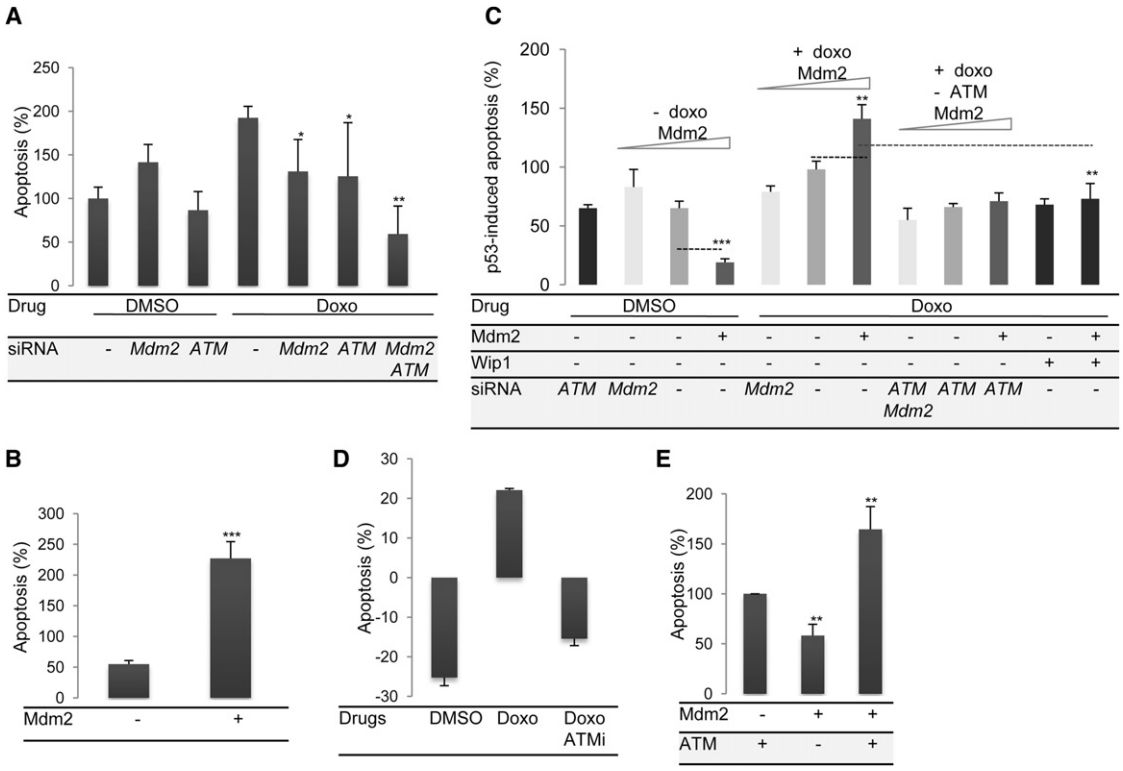

Figure 1. Mdm2 Is a Positive Regulator of p53 Activity in Response to DNA Damage in an ATM-Dependent Manner

Flow cytometry analyses show the levels of apoptosis in different cell lines treated, or not, with the genotoxic drugs doxorubicin (doxo) (0.1–1 μM for 6–16 hr as indicated below) or etoposide (5 μM for 20 hr).

(A) Suppression of Mdm2 and/or ATM using siRNA in MLS-1765 cells expressing endogenous wild-type p53 (p53wt) after treatment with 1 μM doxo for 8 hr. The data are normalized to the level of apoptosis in DMSO-treated cells with control siRNA (100%).

(B) Etoposide-induced apoptosis in $Mdm2^{-/-}$;$p53^{-/-}$ MEF cells expressing exogenous p53wt with, or without, exogenous Mdm2wt.

(C) The graph shows p53-induced apoptosis in $p53^{-/-}$ H1299 cells expressing exogenous p53wt. The levels of Mdm2 were altered using siRNA to knock down endogenous Mdm2 levels, or by overexpressing (+) Mdm2. p53-dependent apoptosis in DMSO- compared to doxo-treated cells (0.1 μM for 16 hr) is shown. Light bars (lanes 2, 5, and 8) represent low Mdm2 levels in cells treated with Mdm2 siRNA, light gray bars (lanes 3, 6, and 9) represent endogenous Mdm2 levels, and darker gray bars (lanes 4, 7, and 10) are cells overexpressing Mdm2.

(D) The relative levels of p53-dependent apoptosis in the presence of exogenous Mdm2 in H1299 cells treated with doxo (0.1 μM for 16 hr) and ATM inhibitor (ATMi, 10 μM for 20 hr).

(E) The levels of apoptosis in $ATM^{-/-}$ cells (AT5-BIVA) expressing exogenous Mdm2 and/or ATM in the presence of doxo (0.1 μM for 6 hr). The data are normalized to the level of apoptosis in cells expressing endogenous Mdm2 (100%). Data are means ± s.d. of at least three independent experiments (*$p < 0.05$, **$p < 0.01$, ***$p < 0.001$). P values are as compared with doxo and no siRNA (A), no Mdm2 (B and E), and as indicated (C). The data using H1299 cells (C and D) are normalized to the levels of apoptosis in mock-transfected cells (0%).

See also Figure S1.

mRNA-Mdm2 interaction was interrupted (Figure S2C). These results indicate that Mdm2's positive effect on p53 activity during genotoxic stress requires ATM-dependent phosphorylation of Mdm2 on Ser395 and the *p53* mRNA-Mdm2 interaction.

Phosphorylation of Mdm2 at Ser395 by ATM Promotes Its Interaction with the *p53* mRNA

We next tested whether ATM activity affects the *p53* mRNA-Mdm2 interaction. The binding of *p53* mRNA to Mdm2 was analyzed by immunoprecipitation (IP) of Mdm2 followed by quantitative RT-PCR (qRNA-coIP) (Candeias et al., 2008). An approximately three-fold induction in the amount of *p53* mRNA bound to Mdm2 was observed following treatment of cells with doxorubicin. This was prevented by the Mdm2S395A mutation or by treating the cells with ATMi or with the general PI3K inhibitor wortmannin. The *p53* mRNA-Mdm2 interaction was stabilized approximately five-fold by introducing the Mdm2S395D mutation in the absence of doxorubicin. Treatment with doxorubicin had no significant additional effect on the *p53* mRNA-Mdm2 interaction, indicating that the Ser395 site is sufficient and necessary. Mdm2 can also be phosphorylated on Y394 by the ATM substrate c-Abl (Goldberg et al., 2002). However, the binding of the *p53* mRNA to Mdm2S394A in response to genotoxic stress was similar to that of Mdm2wt, indicating that this site plays a minor role in controlling RNA binding and at the same time indicates the regulatory specificity of the Ser395 residue (Figure 3A; Figure S3A, left panel). To further test whether the binding of the *p53* mRNA to Mdm2 is controlled by ATM, we used the AT5-BIVA cells. qRNA-coIP using the 4B2 monoclonal Antibody (mAb), which is indifferent to Mdm2's Ser 395 phosphorylation status, revealed almost no *p53* mRNA bound to Mdm2 in these cells. The introduction of ATM restored *p53*

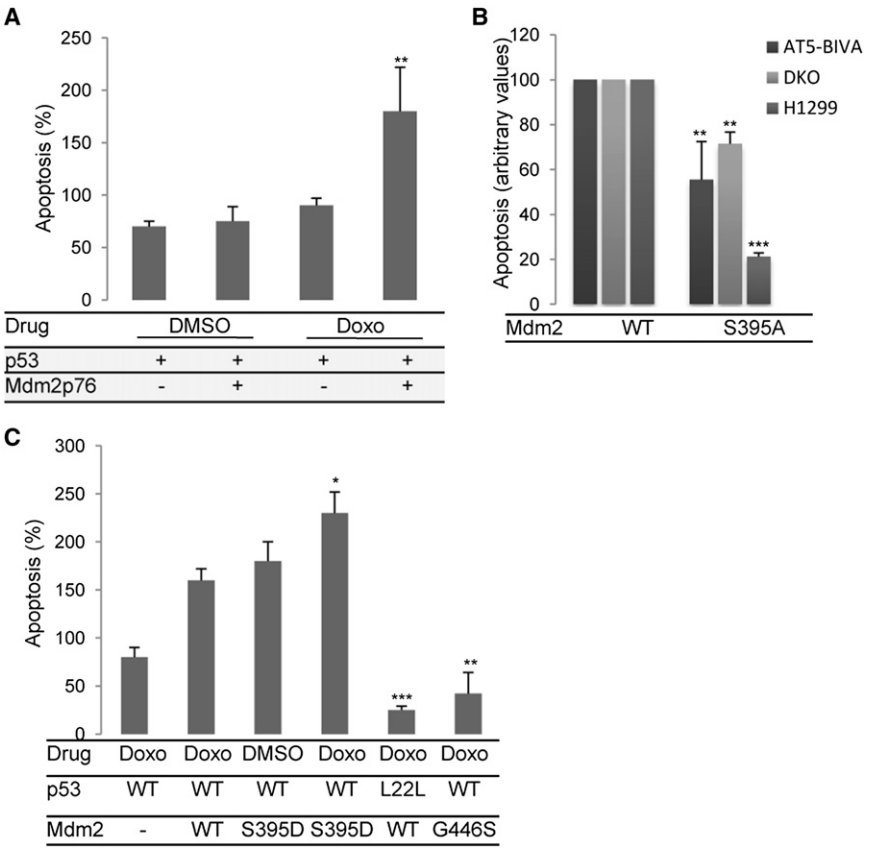

Figure 2. Phosphorylation of Mdm2 at Ser395 Induces p53-Dependent Apoptosis Independently of the p53–Mdm2 Protein-Protein Interaction

(A) The effect of the Mdm2p76 isoform on p53-dependent apoptosis was evaluated in H1299 cells in the presence or absence of genotoxic stress (doxo 0.1 μM for 16 hr). Doxo-treated and nontransfected cells were given the arbitrary value zero.

(B) The effect on p53-dependent apoptosis by Mdm2S395A in the presence of doxo in indicated cells. Cells were transfected with p53wt and with Mdm2wt or Mdm2S395A. The ATM$^{-/-}$ cells (AT5-BIVA) were also transfected with ATM. Apoptosis in the presence of Mdm2wt, p53wt and doxorubicin was given the arbitrary value 100. Mdm2$^{-/-}$;p53$^{-/-}$ double knock-out MEF cells (DKO).

(C) p53-dependent apoptosis in H1299 cells expressing indicated p53 and Mdm2 constructs in the absence, or presence, of doxo. Data are means ± s.d. of at least three independent experiments (*$p < 0.05$, **$p < 0.01$, ***$p < 0.001$). P values are as compared with doxo and no Mdm2 (A), Mdm2wt (B), and Mdm2wt and p53wt (C). The data using H1299 cells (A and C) are normalized to the levels of apoptosis in mock-transfected cells (0%).

See also Figure S2.

mRNA binding to Mdm2, and the affinity of this interaction increased by approximately four-fold after doxorubicin treatment. Importantly, when we instead used the 2A10 mAb, which does not recognize the phosphorylated Ser 395 epitope (Maya et al., 2001), we detected little *p53* mRNA in the qRNA-coIP even in the presence of ATM, indicating that nonphosphorylated Mdm2 has weak affinity to the *p53* mRNA (Figure 3B; Figure S3B). In order to investigate whether ATM-dependent phosphorylation at Mdm2Ser395 regulates Mdm2's binding to the *p53* mRNA, we performed in vitro binding experiments in which ATM immunoprecipitated from cell lysate was added to recombinant Mdm2 purified from Sf9 insect cells and in vitro transcribed *p53* mRNA (Figure S3C). Treatment of cells with doxorubicin prior to cell lysis resulted in an approximately four-fold increase in the amount of *p53* mRNA bound to Mdm2. This increase was suppressed by more than 50% if ATMi or wortmannin were added to the reaction mixture. We also tested the low-affinity *p53L22L* mRNA under these in vitro conditions and found that its interaction with Mdm2 in response to doxorubicin treatment was less than half of that of the wild-type message (Figure 3C). Furthermore, the ATM-dependent increase in the binding of *p53* mRNA to Mdm2 in vitro could be detected using the 4B2 but not the 2A10 mAb (Figure 3D).

Mdm2 is mainly detected in the nucleus in response to stress, but Mdm2-dependent synthesis and degradation of p53 takes place in the cytoplasm, so we wanted to know where the *p53* mRNA-Mdm2 interaction takes place. To address this question, we deleted the nuclear localization signal in Mdm2 (Mdm2ΔNLS). Interestingly, this protein is restricted to the cytoplasmic compartment and binds the *p53* mRNA in vitro (O'Keefe et al., 2003 and data not shown) but it only interacts with a fraction of the *p53* mRNA, as compared with the Mdm2wt, indicating that the *p53* mRNA-Mdm2 interaction mainly takes place in the nucleus (Figure 3E; Figure S3A, right panel).

We further characterized the *p53* mRNA-Mdm2 interaction using a biotinylated oligonucleotide corresponding to the Mdm2-binding sequence of *p53* mRNA (MBD-ES) and purified recombinant Mdm2 proteins expressed in bacteria (Figure S3D). The Mdm2wt showed low affinity for the *p53* MBD-ES, whereas the phospho-mimetic Mdm2S395D displayed a higher estimated affinity (Kdiss 160 nM) (Figures 3F and 3G). An Mdm2 construct that contains the C-terminal residues 322–491, Mdm2(322-491), showed a similar behavior as the full-length Mdm2 protein in that the 395D mutation enhances the RNA-binding capacity. However, a construct including the RING domain, but not Ser395, Mdm2(396-491), showed a similar affinity (Kdiss 400 nM) for the RNA as MdmS2395D, indicating that the RING domain alone is sufficient to bind the *p53* mRNA (Figure 3H). These results suggest that the RNA-binding capacity of Mdm2 takes place in the nuclear compartment and is located to the RING domain of Mdm2 and that the 395 residue is not part of the direct contact with the *p53* mRNA. This also indicates that phosphorylation of Ser395 by ATM promotes Mdm2's RNA-binding capacity via allosteric changes within the C terminus of Mdm2.

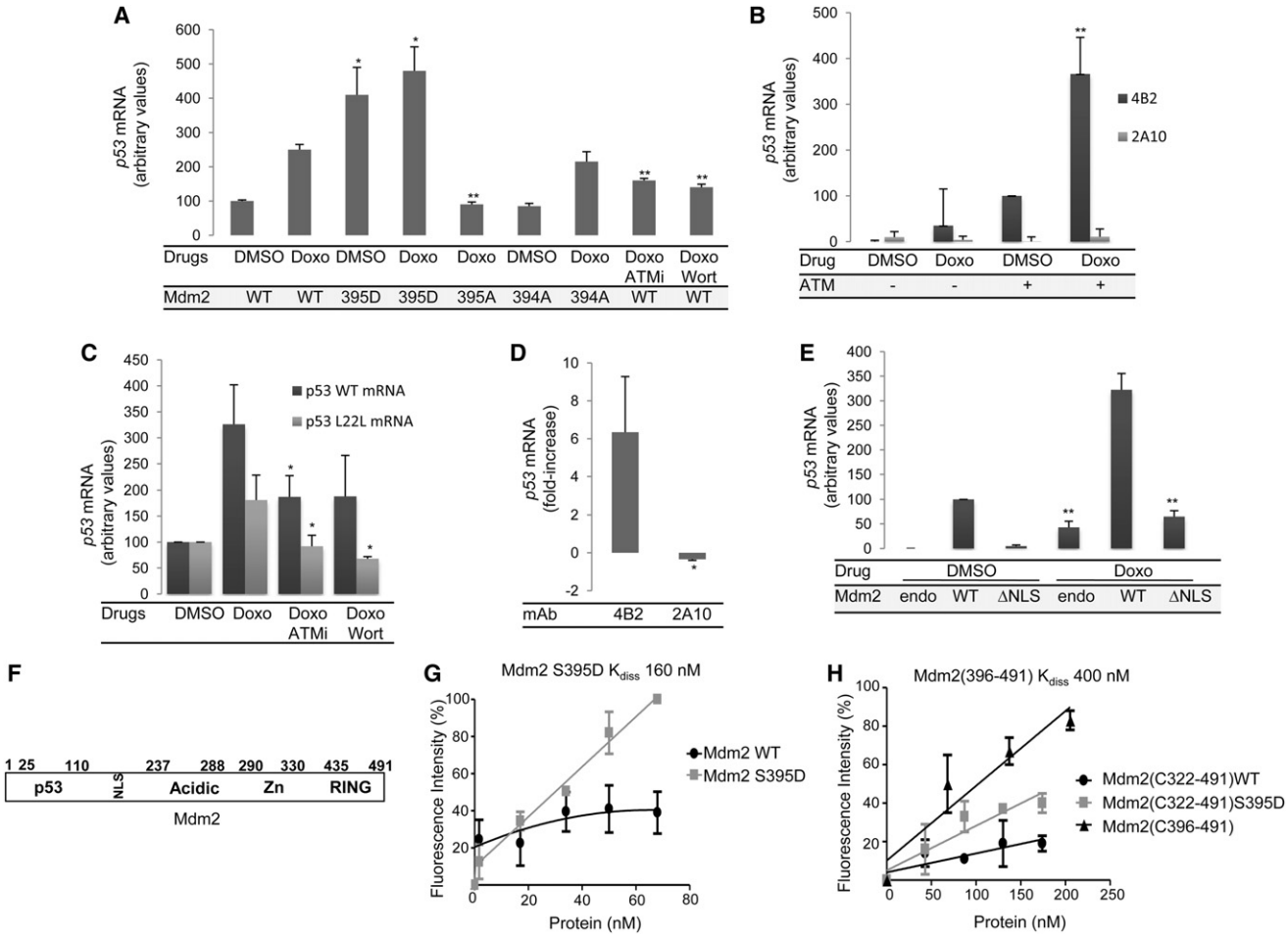

Figure 3. The Binding of the *p53* mRNA to Mdm2 Is Dependent on ATM Activity

(A) The binding of indicated Mdm2 constructs to the p53 mRNA in H1299 cells as estimated using qRNA-coIP. Cells (A–E) were treated with doxo (1 μM for 3 hr) or DMSO. ATM inhibitor (ATMi 10 μM) or the PI3K inhibitor wortmannin (wort. 5 μM) was added for 20 hr before RNA binding was determined.

(B) The binding of *p53* mRNA to Mdm2 in the ATM null AT5-BIVA cells with, or without, exogenous ATM using qRNA-coIP. The anti-Mdm2 monoclonal antibody (mAb) 4B2 is indifferent to phosphorylation, whereas 2A10 does not recognize the phosphorylated Ser395 Mdm2 epitope.

(C) ATM immunoprecipitated from H1299 cells treated, or not, with doxo was added to recombinant purified Mdm2 from Sf9 insect cells and in vitro-synthesized *p53wt* or *p53L22L* mRNAs in the presence or absence of ATMi (10 μM) or wortmannin (5 μM), and the amount of *p53* mRNA bound to Mdm2 was estimated following qRNA-coIP.

(D) ATM-dependent changes in the in vitro binding of *p53* mRNA to Mdm2 as in (C) using 4B2 and 2A10 mAbs.

(E) The binding of Mdm2 wild-type (WT) to the *p53* mRNA in H1299 cells or to an Mdm2 that lacks the nuclear localization signal (ΔNLS) as estimated using qRNA-coIP.

(F) Cartoon illustrating different domains of Mdm2.

(G) In vitro purified recombinant Mdm2wt or Mdm2S395D expressed in bacteria were tested for their binding to in vitro synthesized *p53* mRNA using RNA-ELISA.

(H) In vitro purified truncated recombinant Mdm2 proteins expressed in bacteria were tested for their binding to in vitro synthesized *p53* mRNA using RNA-ELISA.

Data are means ± s.d. of three independent experiments (*$p < 0.05$, **$p < 0.01$, ***$p < 0.001$). P values are as compared with Doxo and Mdm2wt (A, E), no Doxo and ATM (B), Doxo alone (C) and mAb 4B2 (D).

See also Figure S3.

The *p53* mRNA Is Required for Mdm2 SUMO-Conjugation and Nuclear Trafficking

After DNA damage, Mdm2 localizes to nucleoli and this plays an important role in p53's capacity to respond to DNA damage (Lohrum et al., 2000; Weber et al., 1999). Mdm2 also interacts with PML that is linked to RNA transport, and we tested whether the *p53* mRNA plays a role in Mdm2 nuclear translocation (Bernardi et al., 2004; Cohen et al., 2001; Ideue et al., 2004; Kurki et al., 2003). Treatment of p53wt-expressing cells with doxorubicin resulted in the localization of Mdm2 to nucleoli in conjunction with PML nuclear bodies, as reported previously (Figure 4A, top two rows; Figure S4) (Bernardi et al., 2004; Kurki et al., 2003). Interestingly, the localization of Mdm2 to nucleoli after genotoxic stress was abrogated by suppressing the interaction between Mdm2 and the *p53* mRNA using mutants Mdm2S395A or *p53L22L* (Figure 4A, lower panel). The expression of a silent p53 construct (*Sp53* mRNA) lacking initiation codons and that expresses no p53 protein (Candeias et al., 2008) revealed that

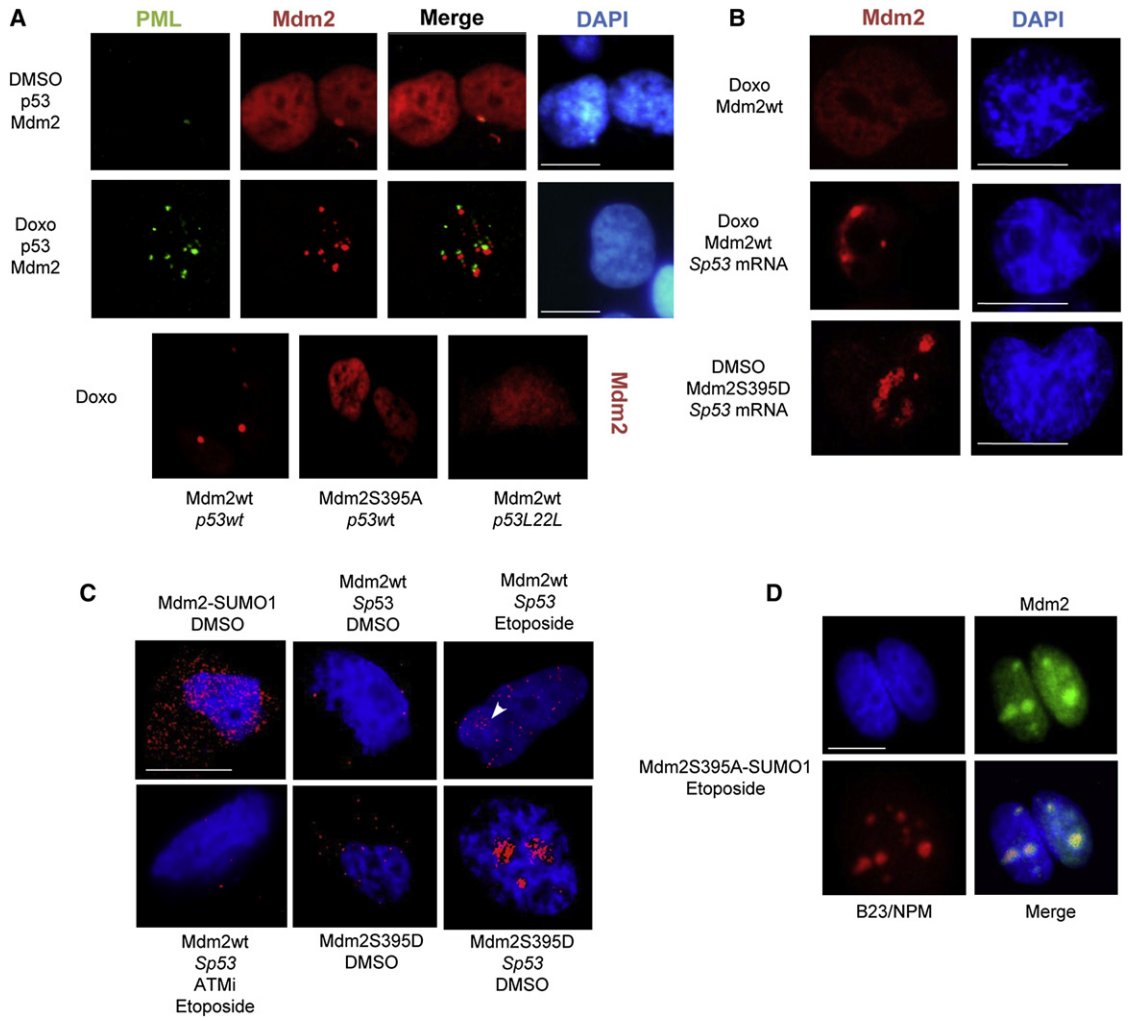

Figure 4. The *p53* mRNA Regulates Mdm2 SUMOylation and Nuclear Trafficking

H1299 cells were transfected with indicated constructs and Mdm2, PML, or B23/NPM was detected by indirect immunofluorescence microscopy staining. Cell nuclei were visualized with DAPI (blue). Fields were merged to assess protein colocalization.

(A) Cells expressing indicated p53 and Mdm2 constructs and treated with DMSO (upper panels) or doxo (middle panels) and stained for PML (green) and Mdm2 (red). The lower panels show staining of Mdm2 in cells overexpressing indicated Mdm2 and p53 constructs after treatment with doxo.

(B) Mdm2 staining in cells expressing indicated constructs and treated with doxo or DMSO.

(C) DuoLink using anti-SUMO1/2 and anti-Mdm2 specific mAbs. Fusion of SUMO1 to Mdm2 (Mdm2-SUMO1) serves as a positive control (upper left). Mdm2 conjugated to endogenous SUMO1/2 is shown in the other slides. Treatment with etoposide leads to an accumulation of SUMOylated Mdm2wt products in nucleoli (white arrow, top right).

(D) Double staining for Mdm2 using 4B2 mAb and anti-B23/NPM polyclonal sera. Data represent three similar independent experiments. Scale bars correspond to 10 μm.

See also Figure S4.

the *p53* mRNA, but not the p53 protein, is required for the nucleolar localization of Mdm2 following genotoxic stress. We also observed that the phosphomimetic S395D mutation resulted in an Mdm2 that, in the presence of the *Sp53* mRNA, localized to the nucleoli in the absence of genotoxic stress (Figure 4B).

SUMO modifications can play a role in nucleolar and PML-related nuclear trafficking, and we used the DuoLink method, which gives a single signal if two different antibody epitopes are localized within 40 nm of each other, to detect and visualize SUMO-conjugated Mdm2 under normal or genotoxic stress conditions. By using antibodies toward Mdm2 and SUMO, we could confirm positive signals throughout the cells using a control Mdm2-SUMO1 fusion construct. Mdm2 wild-type protein was weakly SUMOylated throughout nontreated cells in the presence of p53. Treating cells with etoposide (doxorubicin interferes with the DuoLink signal) in the presence of *Sp53* mRNA resulted in an increase in SUMOylated Mdm2 throughout the nucleus and an accumulation in nucleoli. This was prevented if the cells were treated with the ATMi. Introducing the S395D mutation resulted in an increase in the number of Mdm2-SUMO interactions in nontreated cells. Importantly, when the *Sp53* mRNA was coexpressed with the Mdm2S395D, the SUMOylation of Mdm2 in

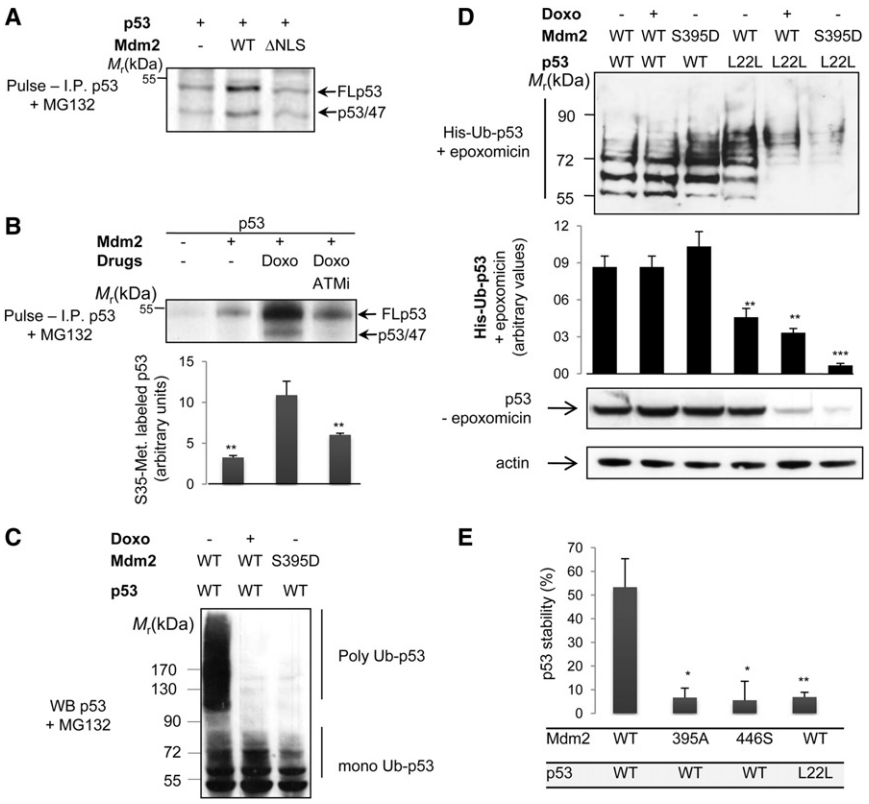

Figure 5. DNA Damage Stimulates ATM-Dependent *p53* mRNA Translation and p53 Polyubiquitination and Degradation

(A) Autoradiograph of a metabolic pulse label in H1299 cells expressing p53 and Mdm2wt or Mdm2ΔNLS in the presence of proteasome inhibitor (MG132 20 μM for 2 hr) followed by p53 IP.

(B) Metabolic pulse-label reveals synthesis of p53 in H1299 cells transfected with indicated constructs and treated, or not, with doxo (0.1 μM for 10 hr) and the specific ATM inhibitor (ATMi; 10 μM for 20 hr).

(C) Cells expressing indicated p53 and Mdm2 constructs were treated, or not, with doxo, and the p53 ubiquitination patterns were visualized after separation on a 7% SDS gel and blotted against p53 CM-1 polyclonal sera. Mono- and polyubiquitinated p53 forms are indicated.

(D) Cells were transfected with ubiquitin-His tag cDNA and indicated constructs in the presence or absence of genotoxic stress. Cells were treated with the proteasome inhibitor epoxomicin (5 μM 4 hr). Upper panel shows lower-molecular-weight ubiquitin-His conjugated p53 proteins after enrichment on Ni-Agarose beads, separated on SDS gels and blotted against p53 (CM-1 pAb). The graph below shows the relative values of three independent experiments as determined by ECL reader. Bottom panels shows corresponding p53 steady state levels (no proteasome inhibitors) and actin loading control.

(E) The graph shows the relative changes in p53 stability in the presence of indicated Mdm2 and p53 constructs after doxo treatment (0.1 μM for 10 hr) followed by cycloheximide for 1 hr prior to lysis. p53 levels in the absence of exogenous Mdm2 was set to 100%. Data are representative of three similar independent experiments and are expressed as means ± s.d. (*p < 0.05, **p < 0.01, ***p < 0.001). P values are as compared with doxo alone (B) and Mdm2wt and p53wt (E) and *p53wt* mRNA (D). See also Figure S5.

nontreated cells was enhanced over 10-fold and restricted to the nucleoli (Figure 4C). We also tested whether conjugation of SUMO1 to Mdm2 plays a direct role in the accumulation of Mdm2 in the nucleolus. Fusion of SUMO1 to Mdm2S395A (Mdm2S395A-SUMO1) resulted in a localization of the fusion protein to the nucleoli under stress conditions and without the presence of *p53* mRNA (Figure 4D). These results show that the *p53* mRNA plays an important role in directing Mdm2 SUMO modification and its nuclear trafficking.

ATM and the *p53* mRNA-Mdm2 Interaction Are Required to Induce p53 Expression following Genotoxic Stress

The binding of the *p53* mRNA to Mdm2 has been shown to promote p53 synthesis. Metabolic pulse-label experiments in the presence of proteasome inhibitors showed that the Mdm2 protein, which lacks the nuclear localization sequence (ΔNLS), does not support p53 synthesis (Figure 5A). This indicates that, even though synthesis of p53 takes place in the cytoplasm, the *p53* mRNA-Mdm2 interaction needs first to take place in the nucleus (Figure 3E). In line with the observation that ATM activity promotes the interaction between the *p53* mRNA and Mdm2, we found that Mdm2 induces more than three-fold increase in the rate of p53 synthesis after cells were exposed to doxorubicin, as compared to nontreated cells. This increase was suppressed by more than 60% if the cells were also treated with the ATMi. The induction of p53 synthesis by endogenous Mdm2 after doxorubicin treatment is approximately 50% (Figure 5B; Figure S5).

The degradation of p53 by Mdm2 involves p53 polyubiquitination, and managing Mdm2's E3 ligase activity toward p53 following DNA damage is important for p53 activation (Li et al., 2003; Thrower et al., 2000). The binding of the *p53* mRNA to the RING domain of Mdm2 can control Mdm2 E3 ligase activity (Candeias et al., 2008; Linares and Scheffner, 2003), we therefore investigated how Mdm2Ser395 phosphorylation and *p53* mRNA binding affects p53 ubiquitination. Treating cells with proteasome inhibitors prior to lysis revealed that the Mdm2-dependent polyubiquitination of p53 is compromised in cells treated with doxorubicin or when the 395D mutation is introduced in Mdm2 (Figure 5C). Monoubiquitination of p53, which can take place on several lysine residues, was relatively unaffected. We also enriched ubiquitinated p53 by expressing a His-ubiquitin construct followed by Ni^{+}-agarose purification. Using either method, we could not detect Mdm2-dependent polyubiquitinated p53 when p53wt protein was expressed from the *L22L* mRNA, but we could detect Mdm2-dependent His-ubiquitinated p53 of less than 90 kD (Figure 5D, upper and middle panel). Importantly, in the presence of genotoxic stress, or by introducing the 395D mutation in Mdm2, we observed a significant reduction in the amount of His-ubiquitinated p53 products of lower molecular weight when the p53wt protein was expressed from the *L22L* mRNA, as compared to the *p53wt*

mRNA, for which the ubiquitination pattern was relatively unchanged under these conditions. At the same time, we observed a sharp decrease in the steady-state levels of p53wt protein expressed from the *p53L22L* mRNA in the presence of either Mdm2S395D or Mdm2wt plus doxorubicin. The levels of p53wt protein expressed from the *p53wt* mRNA increased under these conditions (Figure 5D, lower panels). This shows that p53wt protein expressed from a non-Mdm2 binding mRNA is hyperunstable in the presence of Mdm2 during genotoxic stress. The importance of the *p53* mRNA-Mdm2 interaction in preventing p53 degradation following genotoxic stress was further underlined by introducing the Mdm2G446S and the Mdm2395A mutants, which both have a low affinity for the *p53wt* mRNA. Following doxorubicin and cycloheximide treatment (1 hr), we observed an approximately five-fold higher p53 turnover rate in cells expressing a dysfunctional combination of the *p53* mRNA-Mdm2 interaction (Figure 5E). These results support the notion that the increase in the *p53* mRNA-Mdm2 binding following genotoxic stress leads to both an increase in Mdm2-dependent p53 synthesis and a decrease in Mdm2-dependent degradation p53.

DISCUSSION

The results presented here describe the molecular mechanisms underlying ATM-dependent regulation of Mdm2 nuclear trafficking and p53 activation following genotoxic stress and offer an additional view on p53-dependent induction of Mdm2 expression. Our results support a model in which the induction of the *p53* mRNA-Mdm2 interaction takes place in the nuclear compartment in response to genotoxic stress via ATM-dependent phosphorylation of Mdm2 at Ser395. This event leads to a change of conformation in the Mdm2 RING domain that exposes the binding site for the *p53* mRNA. This, in turn, promotes Mdm2 SUMOylation and brings Mdm2 to the nucleolus and switches Mdm2 into a positive regulator of p53 by increasing p53 synthesis and, at the same time, suppresses Mdm2-dependent degradation of p53. When the DNA damage signaling cascade is turned off, ATM activity ceases and Mdm2 phosphorylation is reversed by Wip1 so that Mdm2 no longer binds the *p53* mRNA and switches to become a negative regulator of p53 activity by promoting p53 polyubiquitination and degradation (Figure 6). Disruption of the *p53* mRNA-Mdm2 interaction leads to a rapid decrease in p53 levels and to a failure in p53 activation in response to genotoxic stress.

Our results show that Mdm2p76 is a positive regulator of p53 activity in response to DNA damage, despite lacking the p53 interactive N-terminal domain, demonstrating that disrupting the p53-Mdm2 protein-protein interaction by ATM-dependent modifications of the p53 N terminus, or on Mdm2, are not required to induce p53 activity following ATM activation. Preventing the p53-Mdm2 protein-protein interaction could help to explain how ATM neutralizes the negative effect of Mdm2 but it cannot explain how Mdm2 actually stimulates p53 activity following genotoxic stress. Our data suggest that, in addition to preventing Mdm2-dependent degradation of p53, the *p53* mRNA-Mdm2 interaction also stimulates p53 synthesis and together these two effects can account for the positive outcome of Mdm2 on p53 expression and activity in response to DNA damage. The activation of p53 via DNA damaged-induced modifications on the p53 N terminus have been suggested, but we observed only a relative small additive effect on p53-dependent apoptosis after doxorubicin treatment in the presence of Mdm2S395D, as compared to the differences observed using the Mdm2wt. No significant difference with or without doxorubicin was found when we knock out Mdm2 in cells expressing endogenous p53wt. This indicates that under these conditions ATM-mediated phosphorylation of p53 plays a less important role in activating p53.

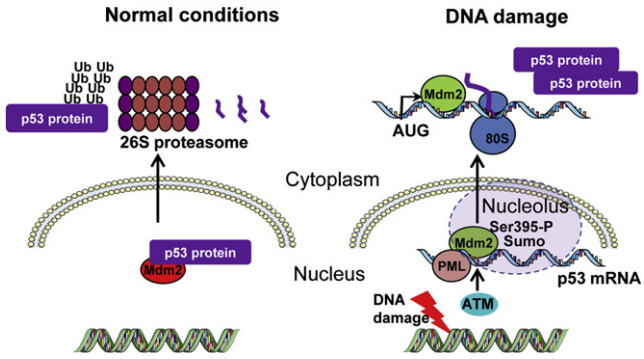

Figure 6. A Model for p53 Activation via ATM-Mdm2 in Response to Genotoxic Stress

Under normal conditions, Mdm2 translocates the p53 protein out of the nucleus for degradation via the ubiquitin-dependent pathway. Under conditions of genotoxic stress, ATM phosphorylates Mdm2 at Ser395. This results in allosteric changes in the C terminus of Mdm2 and opens up the Mdm2 RING domain for *p53* mRNA binding, which, in turn, promotes Mdm2 SUMO-conjugation and its accumulation in the nucleolus. The *p53* mRNA-Mdm2 interaction stimulates *p53* mRNA translation and suppresses Mdm2 E3 ligase activity toward p53 and is required for p53 activation following DNA damage. Suppressing the *p53* mRNA interaction, via either a single silent point mutation in the *p53* mRNA (p53L22L) or an amino acid substitution in Mdm2 (Mdm2S395A), leads to a decrease in p53 levels upon genotoxic stress and a failure to activate the p53 pathway. These results illustrate the importance of the *p53* mRNA in the genotoxic stress pathway and how it controls the activity of Mdm2 toward the p53 protein and offers an explanation to why Mdm2 is upregulated by p53 in response to DNA damage.

It is interesting to notice that expression of a p53wt protein from the *L22L* mRNA with low affinity for Mdm2, or expression of the wild-type *p53* mRNA in the presence of the non-RNA-binding Mdm2S395A mutant, results in an increase in p53 turnover rate following genotoxic stress, as compared to the stabilization observed using *p53wt* mRNA and Mdm2wt. More recently, it was suggested that phosphorylation of the C terminus of Mdm2 induces its monomerization and prevents p53 polyubiquitination (Cheng et al., 2009). Our results do not go against this model, but they show that the phosphorylation of Ser395 induces the *p53* mRNA-Mdm2, interaction which is necessary to inhibit p53 polyubiquitination. The molecular mechanism of the *p53* mRNA-mediated control of Mdm2 E3 ligase activity is not clear and might include a direct interference with the ligase activity, disruption of Mdm2 dimerization, or the interaction with proteins interacting with the C terminus of Mdm2, such as the ubiquitin protease HAUSP (Cummins et al., 2004; Li et al., 2004, 2002).

The localization of Mdm2 to the nucleoli is an important step in p53 activation, and the observation that Mdm2 requires

phosphorylation of Ser395 and the interaction with the *p53* mRNA to locate to nucleolar structures following genotoxic stress further adds to the important role of the *p53* mRNA in controlling Mdm2 functions. The RNA-binding capacity of other nucleolar factors such as nucleolin and NRF have been suggested to play a role in their respective nucleolar accumulation (Emmott and Hiscox, 2009; Niedick et al., 2004), suggesting that RNA-directed nucleolar trafficking is a more widespread concept. The requirement for Ser395 phosphorylation and *p53* mRNA-binding in order to translocate Mdm2 to the nucleolus becomes redundant if SUMO1 is conjugated to Mdm2, indicating that these two events precede SUMO-modification and translocation. In support of the idea that phosphorylation of Ser395 is the first step in this chain of events, we observed that the Mdm2S395D mutant does not localize to the nucleolus following genotoxic stress in the absence of the *p53* mRNA. Because phosphorylation of Ser395 is required for Mdm2's interaction with the *p53* mRNA in vitro and the Mdm2S395D binds *p53* mRNA with higher affinity in the cell, it is unlikely that *p53* mRNA binding to Mdm2 would be an indirect effect of SUMO-conjugation. The role of Mdm2-interacting factors in *p53* mRNA-mediated localization of Mdm2 to the nucleoli will be addressed separately (Poyurovsky et al., 2003; Tao and Levine, 1999).

Mdm2 binds to a region of the *p53* mRNA that has been shown to contain an IRES sequence (Candeias et al., 2008; Gu et al., 2009; Ray et al., 2006). Mdm2 requires nuclear localization to bind the *p53* mRNA and promote *p53* mRNA translation during genotoxic stress, indicating that the accumulation of Mdm2 in the nucleolus serves an important function in assembling the *p53* mRNA-Mdm2 translation complex. Because eukaryotic IRES *trans*-activating factors (ITAFs) are known to shuttle between nucleus and cytoplasm, and some to require expression in the nuclear compartment in order to promote translation in response to cellular stresses, it is possible that the *trans*-localization of Mdm2 within the nucleus to support synthesis of p53 during genotoxic stress reflects a more general aspects of stress-dependent mRNA translation.

Finally, an interesting aspect of these results is that they offer an explanation to the paradox of the rapid induction of Mdm2 by p53 in response to genotoxic stress (Mendrysa and Perry, 2000). As long as the ATM pathway is active and the interaction with the *p53* mRNA is present, Mdm2 serves as a positive regulator of p53 activity but as soon as this activity ceases, Mdm2 returns to be a negative regulator to ensure the suppression of p53 activity under normal conditions.

EXPERIMENTAL PROCEDURES

Cell Lines, Protein Labeling, and Expression

All cell-based assays were performed in $p53^{-/-}$ H1299, $p53^{WT}$ MLS-1765, $ATM^{-/-}$ AT5-BIVA, or $p53^{-/-}$;$Mdm2^{-/-}$ Double-KO MEF (DKO) cells. For all experiments, transfection efficiency and mRNA levels were verified using reverse transcription quantitative PCR (RT-qPCR). ^{35}S-methionine labeling was performed by culturing cells in methionine-free medium including 2% dialyzed FCS for 1 hr and 20 μM of the proteasome inhibitor MG132 (Merck Biosciences, UK). Cells were transfected using Genejuice (Novagen). Easytag Express Protein Labeling Mix (90 μCi; ^{35}S) (PerkinElmer, Boston, USA) was added for 20 min, and p53 proteins were immunoprecipitated using CM-1 antibody and separated by SDS-PAGE. In vitro transcribed capped mRNAs (Ambion, Austin, TX, USA) were prepared according to the manufacturer's protocol. Quantification of radioactively labeled products was determined using phosphoimager (Amersham) and Storm hardware together with Bio-1D software (Vilber-Lourmat). Cycloheximide (CHX, Calbiochem), Doxorubicin (Sigma), Etoposide (Sigma), ATM Kinase Inhibitor (ATMi, Calbiochem), and wortmannin (Calbiochem) or an equal volume of dimethylsuphoxide (DMSO) were used at the concentrations of 10 μg/ml, 0.1–1 μM (depending on the sensitivity of the cell type), 20 μM, 10 μM, and 5 μM, respectively, for the time durations indicated in the figure legends. CM-1, 4B2, 4B11, 2A10, and 1.2 antibodies were all kind gifts from Borek Vojtesek. siRNAs against Mdm2 and ATM were from QIAGEN and were applied according to the manufacturer's recommendations. Cells were transfected with 0.3 μg cDNA per 6-cm dish unless otherwise stated.

His-Ubiquitin Conjugation

Cells (1×10^6) were seeded on 10-cm tissue culture plates and transfected with 0.8 μg of plasmids encoding Mdm2, 6His-Ubiquitin, and p53. Twenty-eight hours after transfection, cells were treated with 0.1 μM of doxorubicin for 16 hr. Proteasome inhibitor MG-132 (25 μM) was added 4 hr before cells were washed twice with PBS and scraped in 1 ml of lysis buffer (6 M guanidinium-HCl, 0.1 M Na_2HPO_4/NaH_2PO_4, 0.01 M Tris-HCl [pH 8], 0.005 M imidazol, and 0.01 M β-mercaptoethanol). The cells were sonicated twice for 10 sec. After sonication, 4 ml of lysis buffer was added with 75 μl of Ni2+-NTA-agarose beads (Clontech) and was incubated for 4 hr at RT with gently agitation. The beads were washed once at RT in lysis buffers, once in wash buffer (8 M urea, 0.1 M Na_2HPO_4/NaH_2PO_4, 0.01 M Tris-HCl [pH 6.8], 0.005 M imidazol, and 0.01 M β-mercaptoethanol), and twice in wash buffer plus 0.1% Triton X-100. Products were eluted by incubating beads in 75 μl of 0.2 M imidazol, 0.15 M Tris-HCl (pH 6.8), 30% glycerol, 0.72 M β-mercaptoethanol, and 5% SDS for 20 min at RT with gentle agitation. Twenty-five microliters of 4× of Laemmeli buffer were added before being analyzed by western blot.

Flow Cytometry

The measurement of the percentage of apoptotic cells in a population was effectuated as described elsewhere (Vermes et al., 1995). Briefly, transfected cells were stained with annexin V-FITC and 7-Aminoactinomycin D (7-AAD) (Sigma, Missouri, USA) and were analyzed by flow cytometry with an LSR flow cytometer and CellQuest software (Becton Dickinson, San Jose, CA, USA). The test discriminates intact cells ($FITC^-/7\text{-}AAD^-$), apoptotic cells ($FITC^+/7\text{-}AAD^-$) and necrotic cells ($FITC^+/7\text{-}AAD^+$).

Quantitative RNA Coimmunoprecipitation

Quantitative RNA Coimmunoprecipitation (qRNAco-IP) assays were based on a previous protocol (Candeias et al., 2008; Tenenbaum et al., 2002). Briefly, transfected H1299 cells were lysed with a buffer containing RNase OUT (100 U/ml, Invitrogen) and centrifuged, and supernatants were precleared with mouse IgG followed by incubation with one of the monoclonal anti-Mdm2 antibodies: SMP14 (directed against amino-acids [aa] 154–167 of Mdm2), 4B2 (recognizes the N terminus of Mdm2) or 2A10 (directed against aa 393–395, cannot bind to Mdm2 that is phosphorylated at Ser395). The complexes were pulled-down using protein G–Sepharose beads (Amersham) treated with proteinase K (Sigma), and RNA was extracted and purified using TRIzol protocol (Invitrogen). RT-qPCR was performed using primers against p53 and control genes TATA Box-binding protein and β-actin. To ensure valid quantification of RNA binding to Mdm2, standard curves were used to attest for transfection, RT-PCR, and qPCR protocols' efficiency. RT-qPCRs on total RNA were realized, and qRNAco-IP values calculated according to the following formula: (qPCRvalue p53mRNA IP / qPCRvalue p53mRNA total) / (qPCRvalue controlmRNA IP / qPCRvalue controlmRNA total). A western blot anti-Mdm2 was done in parallel, and coimmunoprecipitation data were also normalized against total Mdm2 protein when needed.

In Vitro Quantitative RNA Coimmunoprecipitation

All binding reactions were performed for 15 min at 37°C in a binding buffer containing 50 mM Tris (pH 7.5), 150 mM NaCl, 0.02 mg/ml yeast tRNA, and 0.2 mg/ml BSA. ATM protein was included after being immunoprecipitated from H1299 cells using 10 μg of phosphorylation-specific antibody anti-phospho-ATM (Ser1981) (Millipore). One hundred twenty nanograms of hMdm2 protein purified from insect cells and a fixed amount (8.10^{-3} pmol) of WT or L22L p53 mRNA were used. ATM Kinase Inhibitor (10 μM; ATMi, Calbiochem) or 5 μM of

wortmannin (Calbiochem) were added to the reaction where indicated. After incubation, RNA-protein complexes were pulled-down using monoclonal anti-Mdm2 antibodies 4B2 or 2A10 and protein G beads (Amersham). The unbound fraction was recovered for later analysis, and the bound RNA was treated with proteinase K (Sigma). The bound and free RNA fractions were then extracted and purified using TRIzol protocol (Invitrogen). RT-qPCR was performed on these fractions using primers against p53. The binding results were expressed as a ratio between the bound and the total (bound+free) RNA.

Protein-RNA ELISA Assay

Ninety-six-well plates were coated with streptavidin (100 μg/ml in 0.1 M NaHCO3; 50 μl/well) overnight at 4°C. After incubation, plates were washed six times with 200 μl PBS-T and blocked with 50 μl of 3% BSA and 0.1 μg/ml of streptavidin in PBS overnight at 4°C. The plates were washed four times with 0.1% PBS-Tween. A mix of biotinylated RNA (5 pmol) and different amounts of protein previously incubated in a binding buffer containing 50 mM Tris (pH 7.5), 150 mM NaCl, 0.02 mg/ml yeast tRNA, and 0.2 mg/ml BSA for 30 min at 37°C were added to the plates (50 μl/well) and incubated 1 hr at RT. The plates were washed six times with 200μl/well PBS-T, and the 6His mAB/HRP conjugate (Clontech) in PBS 1:1000 (50 μl/well) was added and incubated for 1 hr at RT. Plates were washed six times with 200 μl/well PBS-T, and 50 μl/well of a mix of ECL was added and luminescence was measured. Biotinylated MS2 RNA oligonucleotide was used as a negative control to RNA binding specificity.

Immunofluorescence and Fluorescence Microscopy

H1299 cells were grown on coverslips and treated as indicated. Cells were fixed in 4% paraformaldehyde for 10 min before permeabilization in PBS containing 0.1% Triton X-100 for 2 min. The antibodies used for immunofluorescence microscopy were anti-PML (rabbit; Abcam), anti-Mdm2 (mouse; 4B2; gift from B. Vojtesek), anti-nucleolin (mouse; Abcam), and anti-SUMO1 anti-SUMO2 (sheep; gift from R.T. Hay). Double staining was performed as indicated. For detection, cells were incubated with Alexa-488-conjugated (Invitrogen) or Cy5-conjugated (Molecular probes) anti-rabbit antibodies and Alexa Fluor-568-conjugated (Invitrogen) or Alexa Fluor-633-conjugated (Invitrogen) anti-mouse antibodies.

Duolink

Duolink (Olink) was performed according to the manufacturer's instructions. Briefly, H1299 cells were grown on coverslips and then fixed in 4% paraformaldehyde for 10 min before permeabilization in PBS containing 0.1% Triton X-100 for 2 min. Cells were then blocked in 3% BSA/BPS and primary antibodies were incubated (anti-Mdm2, anti-SUMO1, and anti-SUMO2). After washing the cells, PLA probes were added, followed by hybridization, ligation, and amplification for 90 min at 37°C. DNA (blue) and Mdm2-SUMO interactions (red) were visualized after incubation with the Detection solution. Slides were analyzed by fluorescence microscopy.

SUPPLEMENTAL INFORMATION

Supplemental Information includes five figures and can be found with this article online at doi:10.1016/j.ccr.2011.11.016.

ACKNOWLEDGMENTS

We thank Niclas Zetterblad for confocal microscopy assistance, K. Komatsu for AT5-BIVA cells, Frank Toledo for Mdm2$^{-/-}$/p53$^{-/-}$ MEFs, Y. Shiloh for ATM, and Y. Minami for Wip1. Anti-p53 and anti-Mdm2 antibodies were a gift from B. Vojtesek, and anti-SUMO1 and -SUMO2 antibodies were from R.T. Hay. This work was supported by INSERM, La Ligue Contre le Cancer, and RECAMO CZ.1.05/2.1.00/03.0101. M.M.C. was supported by JSPS, AXA Research Fund, and Fundação para a Ciência e a Tecnologia of Portugal. M.G. was supported by a research fellowship from Indo-French Centre for the Promotion of Advanced Research (IFCPAR) and from the ARC.

Received: May 23, 2011
Revised: September 15, 2011
Accepted: November 23, 2011
Published: January 17, 2012

REFERENCES

Banin, S., Moyal, L., Shieh, S., Taya, Y., Anderson, C.W., Chessa, L., Smorodinsky, N.I., Prives, C., Reiss, Y., Shiloh, Y., and Ziv, Y. (1998). Enhanced phosphorylation of p53 by ATM in response to DNA damage. Science *281*, 1674–1677.

Bartek, J., Bartkova, J., and Lukas, J. (2007). DNA damage signalling guards against activated oncogenes and tumour progression. Oncogene *26*, 7773–7779.

Bernardi, R., and Pandolfi, P.P. (2007). Structure, dynamics and functions of promyelocytic leukaemia nuclear bodies. Nat. Rev. Mol. Cell Biol. *8*, 1006–1016.

Bernardi, R., Scaglioni, P.P., Bergmann, S., Horn, H.F., Vousden, K.H., and Pandolfi, P.P. (2004). PML regulates p53 stability by sequestering Mdm2 to the nucleolus. Nat. Cell Biol. *6*, 665–672.

Boulon, S., Westman, B.J., Hutten, S., Boisvert, F.M., and Lamond, A.I. (2010). The nucleolus under stress. Mol. Cell *40*, 216–227.

Candeias, M.M., Malbert-Colas, L., Powell, D.J., Daskalogianni, C., Maslon, M.M., Naski, N., Bourougaa, K., Calvo, F., and Fåhraeus, R. (2008). P53 mRNA controls p53 activity by managing Mdm2 functions. Nat. Cell Biol. *10*, 1098–1105.

Canman, C.E., Lim, D.S., Cimprich, K.A., Taya, Y., Tamai, K., Sakaguchi, K., Appella, E., Kastan, M.B., and Siliciano, J.D. (1998). Activation of the ATM kinase by ionizing radiation and phosphorylation of p53. Science *281*, 1677–1679.

Cheng, Q., Chen, L., Li, Z., Lane, W.S., and Chen, J. (2009). ATM activates p53 by regulating MDM2 oligomerization and E3 processivity. EMBO J. *28*, 3857–3867.

Cohen, N., Sharma, M., Kentsis, A., Perez, J.M., Strudwick, S., and Borden, K.L. (2001). PML RING suppresses oncogenic transformation by reducing the affinity of eIF4E for mRNA. EMBO J. *20*, 4547–4559.

Cummins, J.M., Rago, C., Kohli, M., Kinzler, K.W., Lengauer, C., and Vogelstein, B. (2004). Tumour suppression: disruption of HAUSP gene stabilizes p53. Nature *428*, 486.

Deisenroth, C., and Zhang, Y. (2010). Ribosome biogenesis surveillance: probing the ribosomal protein-Mdm2-p53 pathway. Oncogene *29*, 4253–4260.

Elenbaas, B., Dobbelstein, M., Roth, J., Shenk, T., and Levine, A.J. (1996). The MDM2 oncoprotein binds specifically to RNA through its RING finger domain. Mol. Med. *2*, 439–451.

Emmott, E., and Hiscox, J.A. (2009). Nucleolar targeting: the hub of the matter. EMBO Rep. *10*, 231–238.

Goldberg, Z., Vogt Sionov, R., Berger, M., Zwang, Y., Perets, R., Van Etten, R.A., Oren, M., Taya, Y., and Haupt, Y. (2002). Tyrosine phosphorylation of Mdm2 by c-Abl: implications for p53 regulation. EMBO J. *21*, 3715–3727.

Gu, L., Zhu, N., Zhang, H., Durden, D.L., Feng, Y., and Zhou, M. (2009). Regulation of XIAP translation and induction by MDM2 following irradiation. Cancer Cell *15*, 363–375.

Heun, P. (2007). SUMOrganization of the nucleus. Curr. Opin. Cell Biol. *19*, 350–355.

Honda, R., Tanaka, H., and Yasuda, H. (1997). Oncoprotein MDM2 is a ubiquitin ligase E3 for tumor suppressor p53. FEBS Lett. *420*, 25–27.

Ideue, T., Azad, A.K., Yoshida, J., Matsusaka, T., Yanagida, M., Ohshima, Y., and Tani, T. (2004). The nucleolus is involved in mRNA export from the nucleus in fission yeast. J. Cell Sci. *117*, 2887–2895.

Jimenez, G.S., Khan, S.H., Stommel, J.M., and Wahl, G.M. (1999). p53 regulation by post-translational modification and nuclear retention in response to diverse stresses. Oncogene *18*, 7656–7665.

Khanna, K.K., Keating, K.E., Kozlov, S., Scott, S., Gatei, M., Hobson, K., Taya, Y., Gabrielli, B., Chan, D., Lees-Miller, S.P., and Lavin, M.F. (1998). ATM associates with and phosphorylates p53: mapping the region of interaction. Nat. Genet. *20*, 398–400.

Kitagawa, R., and Kastan, M.B. (2005). The ATM-dependent DNA damage signaling pathway. Cold Spring Harb. Symp. Quant. Biol. *70*, 99–109.

Kurki, S., Latonen, L., and Laiho, M. (2003). Cellular stress and DNA damage invoke temporally distinct Mdm2, p53 and PML complexes and damage-specific nuclear relocalization. J. Cell Sci. *116*, 3917–3925.

Lallemand-Breitenbach, V., and de Thé, H. (2010). PML nuclear bodies. Cold Spring Harb. Perspect. Biol. *2*, a000661.

Li, M., Chen, D., Shiloh, A., Luo, J., Nikolaev, A.Y., Qin, J., and Gu, W. (2002). Deubiquitination of p53 by HAUSP is an important pathway for p53 stabilization. Nature *416*, 648–653.

Li, M., Brooks, C.L., Wu-Baer, F., Chen, D., Baer, R., and Gu, W. (2003). Mono- versus polyubiquitination: differential control of p53 fate by Mdm2. Science *302*, 1972–1975.

Li, M., Brooks, C.L., Kon, N., and Gu, W. (2004). A dynamic role of HAUSP in the p53-Mdm2 pathway. Mol. Cell *13*, 879–886.

Linares, L.K., and Scheffner, M. (2003). The ubiquitin-protein ligase activity of Hdm2 is inhibited by nucleic acids. FEBS Lett. *554*, 73–76.

Lohrum, M.A., Ashcroft, M., Kubbutat, M.H., and Vousden, K.H. (2000). Identification of a cryptic nucleolar-localization signal in MDM2. Nat. Cell Biol. *2*, 179–181.

Lu, X., Nannenga, B., and Donehower, L.A. (2005). PPM1D dephosphorylates Chk1 and p53 and abrogates cell cycle checkpoints. Genes Dev. *19*, 1162–1174.

Lu, X., Ma, O., Nguyen, T.A., Jones, S.N., Oren, M., and Donehower, L.A. (2007). The Wip1 Phosphatase acts as a gatekeeper in the p53-Mdm2 autoregulatory loop. Cancer Cell *12*, 342–354.

Maya, R., Balass, M., Kim, S.T., Shkedy, D., Leal, J.F., Shifman, O., Moas, M., Buschmann, T., Ronai, Z., Shiloh, Y., et al. (2001). ATM-dependent phosphorylation of Mdm2 on serine 395: role in p53 activation by DNA damage. Genes Dev. *15*, 1067–1077.

Mendrysa, S.M., and Perry, M.E. (2000). The p53 tumor suppressor protein does not regulate expression of its own inhibitor, MDM2, except under conditions of stress. Mol. Cell. Biol. *20*, 2023–2030.

Naski, N., Gajjar, M., Bourougaa, K., Malbert-Colas, L., Fåhraeus, R., and Candeias, M.M. (2009). The p53 mRNA-Mdm2 interaction. Cell Cycle *8*, 31–34.

Niedick, I., Froese, N., Oumard, A., Mueller, P.P., Nourbakhsh, M., Hauser, H., and Köster, M. (2004). Nucleolar localization and mobility analysis of the NF-kappaB repressing factor NRF. J. Cell Sci. *117*, 3447–3458.

O'Keefe, K., Li, H., and Zhang, Y. (2003). Nucleocytoplasmic shuttling of p53 is essential for MDM2-mediated cytoplasmic degradation but not ubiquitination. Mol. Cell. Biol. *23*, 6396–6405.

Ofir-Rosenfeld, Y., Boggs, K., Michael, D., Kastan, M.B., and Oren, M. (2008). Mdm2 regulates p53 mRNA translation through inhibitory interactions with ribosomal protein L26. Mol. Cell *32*, 180–189.

Oliner, J.D., Pietenpol, J.A., Thiagalingam, S., Gyuris, J., Kinzler, K.W., and Vogelstein, B. (1993). Oncoprotein MDM2 conceals the activation domain of tumour suppressor p53. Nature *362*, 857–860.

Perry, M.E. (2004). Mdm2 in the response to radiation. Mol. Cancer Res. *2*, 9–19.

Poyurovsky, M.V., Jacq, X., Ma, C., Karni-Schmidt, O., Parker, P.J., Chalfie, M., Manley, J.L., and Prives, C. (2003). Nucleotide binding by the Mdm2 RING domain facilitates Arf-independent Mdm2 nucleolar localization. Mol. Cell *12*, 875–887.

Ray, P.S., Grover, R., and Das, S. (2006). Two internal ribosome entry sites mediate the translation of p53 isoforms. EMBO Rep. *7*, 404–410.

Shieh, S.Y., Ikeda, M., Taya, Y., and Prives, C. (1997). DNA damage-induced phosphorylation of p53 alleviates inhibition by MDM2. Cell *91*, 325–334.

Shiloh, Y. (2003). ATM and related protein kinases: safeguarding genome integrity. Nat. Rev. Cancer *3*, 155–168.

Shreeram, S., Demidov, O.N., Hee, W.K., Yamaguchi, H., Onishi, N., Kek, C., Timofeev, O.N., Dudgeon, C., Fornace, A.J., Anderson, C.W., et al. (2006). Wip1 phosphatase modulates ATM-dependent signaling pathways. Mol. Cell *23*, 757–764.

Tao, W., and Levine, A.J. (1999). P19(ARF) stabilizes p53 by blocking nucleo-cytoplasmic shuttling of Mdm2. Proc. Natl. Acad. Sci. USA *96*, 6937–6941.

Tenenbaum, S.A., Lager, P.J., Carson, C.C., and Keene, J.D. (2002). Ribonomics: identifying mRNA subsets in mRNP complexes using antibodies to RNA-binding proteins and genomic arrays. Methods *26*, 191–198.

Thrower, J.S., Hoffman, L., Rechsteiner, M., and Pickart, C.M. (2000). Recognition of the polyubiquitin proteolytic signal. EMBO J. *19*, 94–102.

Vermes, I., Haanen, C., Steffens-Nakken, H., and Reutelingsperger, C. (1995). A novel assay for apoptosis: flow cytometric detection of phosphatidylserine expression on early apoptotic cells using fluorescein labelled Annexin V. J. Immunol. Methods *184*, 39–51.

Weber, J.D., Taylor, L.J., Roussel, M.F., Sherr, C.J., and Bar-Sagi, D. (1999). Nucleolar Arf sequesters Mdm2 and activates p53. Nat. Cell Biol. *1*, 20–26.

Yoda, A., Toyoshima, K., Watanabe, Y., Onishi, N., Hazaka, Y., Tsukuda, Y., Tsukada, J., Kondo, T., Tanaka, Y., and Minami, Y. (2008). Arsenic trioxide augments Chk2/p53-mediated apoptosis by inhibiting oncogenic Wip1 phosphatase. J. Biol. Chem. *283*, 18969–18979.

Zhu, J., Zhou, W., Jiang, J., and Chen, X. (1998). Identification of a novel p53 functional domain that is necessary for mediating apoptosis. J. Biol. Chem. *273*, 13030–13036.